Bioorganic & Medicinal Chemistry Letters 21 (2011) 2212–2215

Contents lists available at ScienceDirect

Bioorganic & Medicinal Chemistry Letters

journal homepage: www.elsevier.com/locate/bmcl

Investigation of the mode of binding of a novel series of *N*-benzyl-4-heteroaryl-1-(phenylsulfonyl)piperazine-2-carboxamides to the hepatitis C virus polymerase

Robert G. Gentles [a,*], Steven Sheriff [a], Brett R. Beno [a], Changhong Wan [a], Kevin Kish [a], Min Ding [a], Xiaofan Zheng [a], Louis Chupak [a], Michael A. Poss [a], Mark R. Witmer [a], Paul Morin [a], Ying-Kai Wang [b], Karen Rigat [b], Julie Lemm [b], Stacey Voss [b], Mengping Liu [b], Lenore Pelosi [b], Susan B. Roberts [b], Min Gao [b], John F. Kadow [c]

[a] Bristol Myers Squibb, Chemical and Protein Technologies, Wallingford, CT 06492, United States
[b] Bristol-Myers Squibb, Department of Virology, 5 Research Parkway, Wallingford, CT 06492, United States
[c] Bristol Myers Squibb, Medicinal Chemistry, 5 Research Parkway, Wallingford, CT 06492, United States

ARTICLE INFO

Article history:
Received 28 January 2011
Revised 26 February 2011
Accepted 2 March 2011
Available online 6 March 2011

Keywords:
HCV
NS5B
Co-crystal
Structure
Antiviral
Inhibitor
Polymerase

ABSTRACT

Structure based rationales for the activities of potent *N*-benzyl-4-heteroaryl-1-(phenylsulfonyl)piperazine-2-carboxamide inhibitors of the hepatitis C viral polymerase are described herein. These compounds bind to the hepatitis C virus non-structural protein 5B (NS5B), and co-crystal structures of select examples from this series with NS5B are reported. Comparison of co-crystal structures of a potent analog with both NS5B genotype 1a and genotype 1b provides a possible explanation for the genotype-selectivity observed with this compound class and suggests opportunities for the further optimization of the series.

Hepatitis C virus (HCV) RNA-dependent RNA polymerase, also referred to as non-structural protein 5B (NS5B), is responsible for replication of the viral genome and is essential in the life cycle of the virus.[1] Correspondingly, it has long been considered an attractive target for the development of direct acting antiviral (DAA) agents. In recent years a number of reports of both active-site and allosteric NS5B inhibitors have appeared and examples from both inhibitor classes have progressed into clinical evaluation with encouraging initial results.[2]

In an earlier manuscript we described the identification of compound **1** (Fig. 1) from a high throughput screen directed against the NS5B polymerase.[3] In a secondary replicon assay[4] this compound displayed moderate activity against HCV genotype 1b (EC_{50} = 2 μM), but was 10-fold less active (EC_{50} = 25 μM) in a related HCV genotype 1a assay. Exploratory lead optimization led to the identification of significantly more potent analogs such as compound **2**. This molecule displayed EC_{50} values in the replicon 1b and 1a assays of 7 nM and 87 nM, respectively. A notable feature of the structure–activity relationships (SARs) observed during the early development of this series was the consistently enhanced activity against genotype 1b, despite the introduction of significant structural modification.

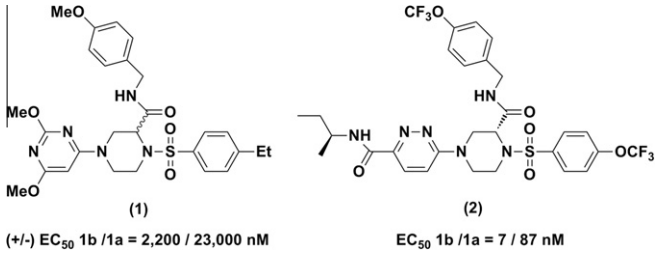

Figure 1. Piperazine based HCV NS5B inhibitors displaying significant selectivity for genotype 1b over genotype 1a. Compound **1** is racemic, and compound **2** has the absolute stereochemistry shown.

* Corresponding author.
E-mail address: robert.gentles@bms.com (R.G. Gentles).

0960-894X/$ - see front matter © 2011 Elsevier Ltd. All rights reserved.
doi:10.1016/j.bmcl.2011.03.011

To provide some insight into this observation, select co-crystal structures were obtained with analogs from this series complexed with the NS5B protein. The structural data proved to be particularly helpful in explaining many aspects of the observed SAR. However, these data were less helpful in identifying specific interactions between the ligands and the NS5B 1b and 1a proteins that could explain the observed genotype selectivity, as discussed below.

In addition to compounds **1** and **2**, co-crystal structures with NS5B were obtained with the analogs **3**, **4** and **5** depicted in Figure 2. The syntheses of all of these compounds have been previously reported,[3,5] and all are accessible by relatively concise synthetic routes.

As discussed in the introduction, compound **1** was identified from a high throughput screen. Subsequent profiling against a panel of mutant NS5B enzymes with point mutations at sites known to bind allosteric inhibitors, suggested that compound **1** most probably bound in the Palm domain of the protein. A co-crystal of **1** bound to NS5B genotype 1b[6a,b] was subsequently obtained and is shown in Figure 3.

This structure confirmed that **1** binds at a largely hydrophobic site at the interface of the palm, fingers and thumb domains. This pocket is exposed by a movement of the C-terminus that allows entry to a cavity that is otherwise inaccessible in the apo structure, (an observation that suggests a degree of dynamism exists in this region of the protein, vide infra).

Interestingly, the 4-ethylbenzenesulfonamide moiety binds in a hydrophobic pocket which is occupied by residues W550 and F551 in the NS5B apo structure (1C2P[8] in the Protein Data Bank[9]). These two residues are part of a C-terminal regulatory motif which modulates the activity of NS5B.[10,11] With respect to specific ligand–protein interactions, the pyrimidine ring of **1** participates in a π-stacking interaction with F193, and the methoxyphenyl ring π-stacks with Y448. The carboxamide moiety of the ligand donates an H-bond to the Y195 backbone carbonyl, and the guanidine moiety of R200 is proximal to the methoxyphenyl ring in the ligand with an NH directed towards the π-face of the ring suggesting a cation–π interaction. The structure suggests that the (*R*)-stereochemistry is required at the chiral center on the piperazine ring, which was confirmed by synthesis using specific piperazine enantiomers.[3] The functionalities projecting from the carboxamide and sulfonamide vectors in **1** are already highly complementary to the cavities into which they project (Fig. 3). Consistent with this observation was the finding that attempts to incorporate significant structural modification at either of these vectors resulted in a notable loss of activity. Despite testing an extensive series of analogs, only modest gains in potency could be achieved, as observed with piperazine **3**. This analog displayed EC_{50} values against genotypes 1b and 1a of 700 nM and 8100 nM, respectively. A co-crystal structure of compound **3** complexed with NS5B genotype 1b was obtained. Piperazine **3** was found to bind in a similar fashion to compound **1** (Fig. 4). Despite the lower resolution of this structure more residues of the NS5B C-terminus were resolved, and L547, W550, F551, Y555, and S556 are proximal to the bound ligand (Fig. 4). A hydrogen bond between a methoxy group on the ligand pyrimidine ring and the backbone NH of G449 is also observed. However, as aromatic ether oxygens are poor hydrogen bond acceptors, this is likely to contribute little to the potency of **3**.

Slightly more extensive van der Waals interactions between the trifluoromethoxy group in **3** and the hydrophobic pocket into which

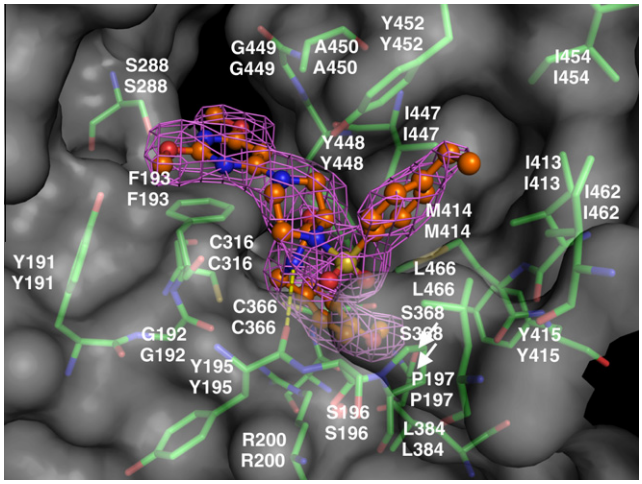

Figure 3. Compound **1** bound to NS5B 1b (Bartenschlager construct).[6c] Figure based on the 2.6 Å resolution co-crystal structure of the ternary complex of NS5B 1b WT with **1** bound and the P495 thumb binding site occupied by a different ligand. In magenta is 1σ $2F_o - F_c$ electron density. Image generated with the PyMOL Molecular Graphics System, Version 1.3, Schrödinger, LLC.[7]

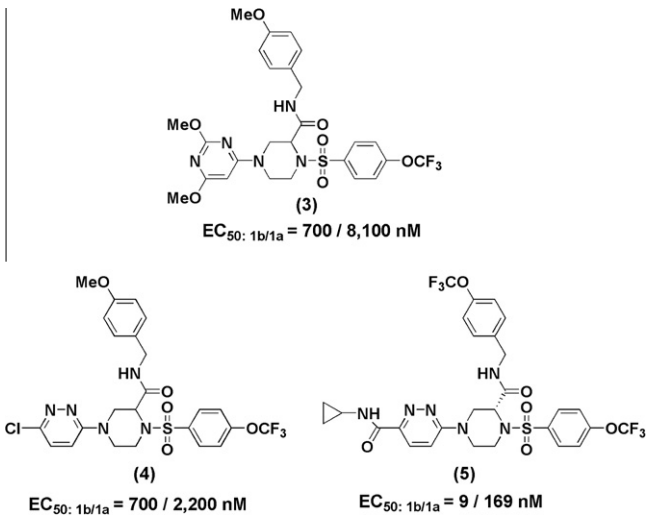

Figure 2. Piperazine based NS5B inhibitors used in co-crystallization studies with HCV NS5B. Compounds were tested as racemates, unless the absolute stereochemistry is depicted.

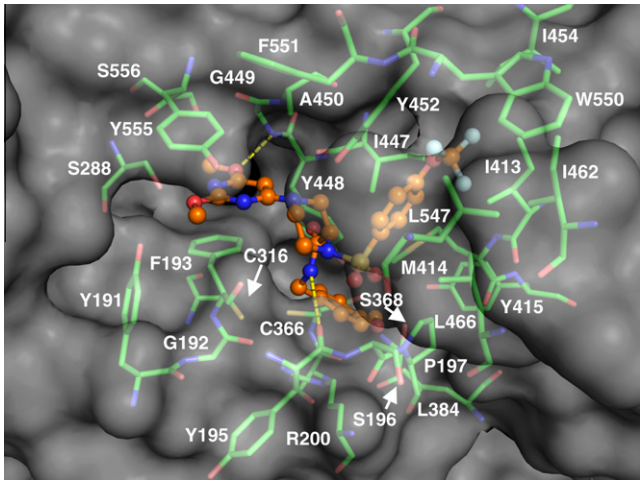

Figure 4. Compound **3** bound to NS5B 1b (Bartenschlager construct).[12] Figure based on the 3.0 Å resolution co-crystal structure of the ternary complex of NS5B 1b WT with **3** bound and the P495 thumb binding site occupied by a different ligand. Image generated with the PyMOL Molecular Graphics System, Version 1.3, Schrödinger, LLC.[7]

the sulfonamide moiety projects probably account for the modest potency improvement observed with this analog relative to **1**.

A notable feature in both complexes is that a significant unoccupied volume exists around the pendant pyrimidine moiety, and as previously reported,[3] the SAR favors pyridazine heterocycles at this position. In order to understand this, a co-crystal structure was obtained with the pyridazine ligand **4** complexed to NS5B genotype 1b (Fig. 5).

Several interesting features in this structure were observed. First, the principal hydrophobic interactions exhibited by the pendant sulfonamide and carboxamide moieties are retained, and the latter maintains a hydrogen bond with the Y195 backbone carbonyl. Second, the pyridazine ring still appears to participate in a π-stacking interaction with F193. The observed EC_{50} values for **4** of 700 nM and 2200 nM against genotypes 1b and 1a, respectively, are similar to those reported for compound **3**. Since **3** and **4** are identical except for the dimethoxypyrimidine in the former, and the chloropyridazine in the latter, it is likely that these two moieties contribute approximately equally to the potency of the respective ligands.

It is apparent from the structure depicted in Figure 5 that 3,6-disubstituted pyridazines with relatively small substituents could be accommodated, and may be associated with enhanced activity. A structure–activity relationship (SAR) study was conducted to determine the optimal moiety at the 6-position of the heterocycle and involved the preparation of a focused array of *N*-alkyl substituted carboxamides. This substitution was associated with a dramatic enhancement of potency, as observed with compound **2** that displayed EC_{50} values against genotypes 1b and 1a of 7 nM and 87 nM, respectively. A co-crystal structure of **2** complexed with NS5B genotype 1b was obtained and is shown in Figure 6. In addition to the previously mentioned interactions, a number of other binding contacts were observed, the most significant being H-bonding between Y555 and S288 and the 6-carboxamide moiety, and additional hydrophobic contacts with the carboxamide *N*-alkyl substituent. One of the pyridazine ring nitrogen atoms also forms water-bridged hydrogen bonds with the protein. Collectively, these interactions could account for the enhanced potency observed for compound **2**.

With potent analogs identified, the origin of the consistent 1b genotype selectivity exhibited by this compound class was explored. Two co-crystal structures were obtained of compound **5** bound to NS5B genotypes 1b and 1a. These structures are depicted in Figures 7 and 8, respectively.

The conformation of **5** in these two complexes is similar. The most significant differences between the structures occur in the vicinity of the carboxamide moiety. However, careful analysis of the geometrically non-optimal H-bonding arrays in this area suggests these differences are unlikely to account for the genotype selectivity exhibited by **5**.

Only a single amino acid difference exists between genotypes 1b and 1a in the region proximal to that occupied by the ligand; a tyrosine is present at position 415 in NS5B 1b, and phenylalanine occupies this position in genotype 1a. It is difficult to rationalize how this sequence change can account for the potency differences observed. Given that this binding site is accessible only on displacement of the C-terminus, it is possible that the dynamics of the NS5B 1b and 1a proteins are different, and could account for the observed potency differences.

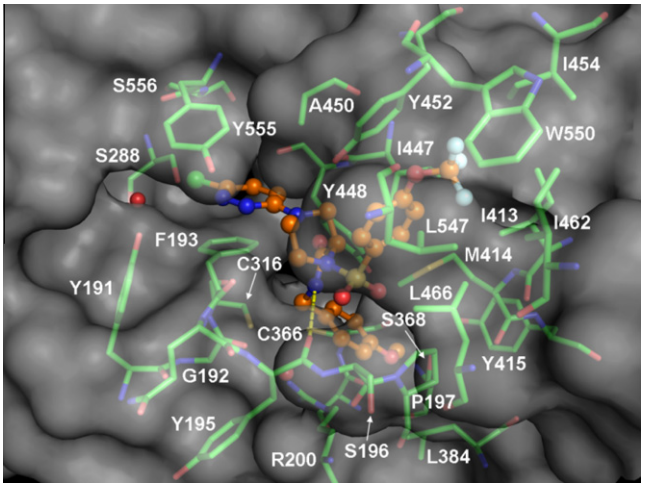

Figure 5. Compound **4** bound to NS5B 1b (Bartenschlager construct).[13] Figure based on the 2.5 Å resolution co-crystal structure of the ternary complex of NS5B 1b with **4** bound and the P495 thumb binding site occupied by a different ligand. Image generated with the PyMOL Molecular Graphics System, Version 1.3, Schrödinger, LLC.[7]

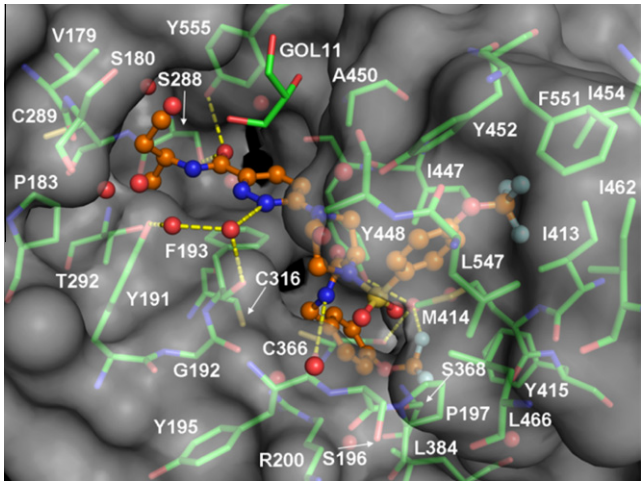

Figure 6. Compound **2** bound to NS5B 1a.[14] Figure based on the 1.8 Å resolution co-crystal structure of NS5B 1a with **2** bound. Image generated with the PyMOL Molecular Graphics System, Version 1.3, Schrödinger, LLC.[7]

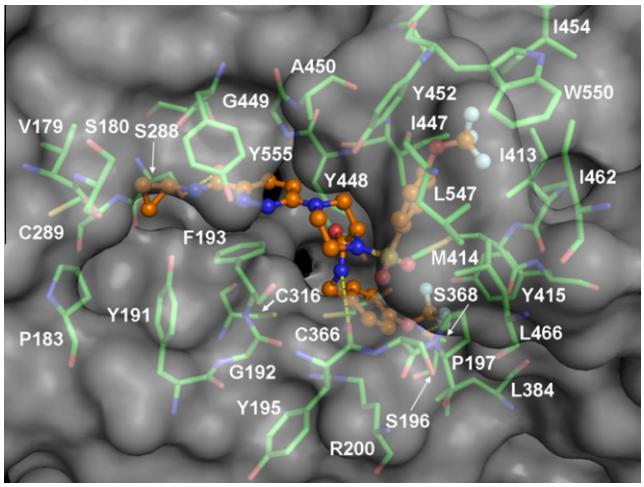

Figure 7. Compound **5** bound to NS5B 1b WT.[15] Figure based on the 3.2 Å resolution co-crystal structure of the ternary complex of NS5B 1b WT with **5** bound and the P495 thumb binding site occupied by a different ligand. Image generated with the PyMOL Molecular Graphics System, Version 1.3, Schrödinger, LLC.[7]

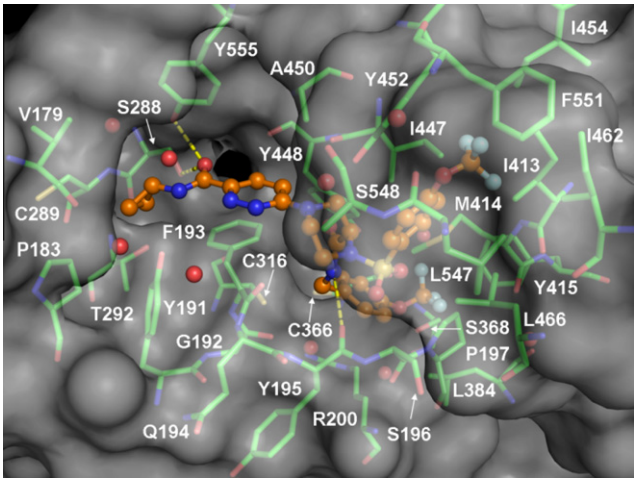

Figure 8. Compound **5** bound to NS5B 1a.[16] Figure based on the 2.1 Å resolution co-crystal structure of NS5B 1a with **5** bound. Image generated with the PyMOL Molecular Graphics System, Version 1.3, Schrödinger, LLC.[7]

Support for this possibility is provided by the fact that part of the binding site for the ligands is occupied by W550 and F551 of the C-terminal regulatory motif in the apo structure of NS5B 1b.[10,11] Along with L447, these residues serve to anchor the C-terminus to the surface of the protein. Interestingly, the two residues flanking W550 and F551 differ in genotypes 1a and 1b (1a: G549, T552; 1b: S549, V552). It may be that these sequence differences modulate the propensity of the C-terminus for displacement or alter the conformational preferences of the C-terminus once it dissociates from the binding site. Alternatively, crystal packing in the two different crystal forms may account for the observed positions of the mobile C-terminal region which may not represent solution conformations. Another possibility is that some interaction(s), as yet unspecified, remote from the binding site may be responsible for the diminished activity observed with the 1a genotype. Unfortunately, on the basis of extant data, it is not possible to be more definitive.

In conclusion, the structures described above clearly rationalize much of the SAR observed with the piperazine class of NS5B inhibitors, although no clear explanation for the observed genotype selectivity has yet emerged. In addition, it is apparent that further optimization of the pendant heteroaryl-carboxamide moiety may be merited, and it would seem reasonable to anticipate improvements in potency that may be sufficient to accommodate the reduced level of activity consistently observed with NS5B 1a genotype.

Acknowledgments

Most of the X-ray data used in this work were collected at the IMCA-CAT beamlines 17-ID (NS5B 1b/compounds **1** and **4**) and 17-BM (NS5B 1a/compound **2**) and at the (SER-CAT) beamlines 22-ID (NS5B 1b/compound **5**) and 22-BM (NS5B 1a/compound **5**) at the Advanced Photon Source, Argonne National Laboratory. IMCA-CAT was supported by the companies of the Industrial Macromolecular Crystallography Association through a contract with the Center for Advanced Radiation Sources at the University of Chicago. Institutions supporting Southeast Regional Collaborative Access Team may be found at www.ser-cat.org/members.html. Use of the Advanced Photon Source was supported by the US Department of Energy, Office of Science, Office of Basic Energy Sciences, under Contract No. W-31-109-Eng-38. Lastly, the authors would like to thank Dr. Carl Bergstrom for his help in reviewing this manuscript.

References and notes

1. Vo, N. V.; Tuler, J. R.; Lai, M. M. C. *Biochemistry* **2004**, *43*, 10579.
2. Powdrill, M. H.; Bernatchez, J. A.; Gotte, M. *Viruses* **2010**, *2*, 2169.
3. Gentles, R. G.; Ding, M.; Zheng, X.; Chupak, L.; Poss, M. A.; Beno, B.; Rigat, K.; Roberts, S.; Gao, M.; Kadow, J. *Bioorg. Med. Chem. Lett.*, in press.
4. (a) Wang, Y.-K.; Rigat, K. L.; Roberts, S. R.; Gao, M. *Anal. Biochem.* **2006**, *359*, 106; (b) Wang, Y.-K.; Rigat, K. L.; Sun, J.-H.; Roberts, S. R.; Gao, M. *Biochem. Biophys.* **2008**, *470*, 146.
5. Abe, H.; Tanaka, M.; Sugimoto, K.; Suma, A.; Yokota, M.; Shiozaki, M.; Iio, K.; Ueyama, K.; Motoda, D.; Noguchi, T.; Adachi, T.; Tsuruha, J.; Doi, S. PCTInt. Appl. WO 2007119889, 2007; *Chem. Abstr.* **2007**, *120*, 4767.
6. (a) Lohmann, V.; Korner, F.; Koch, J.-O.; Herian, U.; Theilmann, L.; Bartenschlager, R. *Science* **1999**, *285*, 110; (b) Wang, Y.-K.; Rigat, K. L.; Roberts, S. B.; Gao, M. *Anal. Biochem.* **2006**, *359*, 106; (c) Compound **1** bound to NS5B 1b, Bartenschlager construct: PDB 3QGD.
7. PyMOL is accessible at www.pymol.org. Ligand atoms are shown in ball and stick representation with orange carbon atoms, red oxygen atoms, blue nitrogen atoms, yellow sulfur atoms, green chlorine atoms and cyan fluorine atoms. Protein residues within 5 Å of the ligand are shown in stick representation with green carbon atoms, red oxygen atoms, blue nitrogen atoms, and yellow sulfur atoms. Water molecules are depicted as red spheres. The surface of the protein within 15 Å of the bound ligand is shown in transparent gray.
8. Lesburg, C. A.; Cable, M. B.; Ferrari, E.; Hong, Z.; Mannarino, A. F.; Weber, P. C. *Nat. Struct. Biol.* **1999**, *6*, 937.
9. Berman, H. M.; Westbrook, J.; Feng, Z.; Gilliland, G.; Bhat, T. N.; Weissig, H.; Shindyalov, I. N.; Bourne, P. E. *Nucleic Acids Res.* **2000**, *28*, 235.
10. Adachi, T.; Ago, H.; Habuka, N.; Okuda, K.; Komatsu, M.; Ikeda, S.; Yatsunami, K. *Biochim. Biophys. Acta Proteins Proteomics* **2002**, *1601*, 38.
11. Leveque, V. J. P.; Johnson, R. B.; Parsons, S.; Ren, J.; Xie, C.; Zhang, F.; Wang, Q. M. *J. Virol.* **2003**, *77*, 9020.
12. Compound **3** bound to NS5B 1b, Bartenschlager construct: PDB 3QGE.
13. Compound **4** bound to NS5B 1b, Bartenschlager construct: PDB 3QGF.
14. Compound **2** bound to NS5B 1a, PDB 3QGI.
15. Compound **5** bound to NS5B 1b, Bartenschlager construct: PDB 3QGG.
16. Compound **5** bound to NS5B 1a, PDB 3QGH.